J Nanostruct 13(2): 431-441, Spring 2023

RESEARCH PAPER

Effect of Si Concentration on Mechanical and Physical Properties of Nano-Size Alkaline-Based Pure Natural Kaolinite

Hasanein A. Mohsien *, Hikmat j. Abdul Baqi

College of dentistry, Department of prosthetic dentistry, University of Baghdad, Baghdad, Iraq

ARTICLE INFO

Article History:
Received 07 January 2023
Accepted 22 March 2023
Published 01 April 2023

Keywords:
Alkaline-Based Activator
Geopolymer
Kaolinite
Meta Kaolinite

ABSTRACT

Geopolymer is a promising material for dental implant abutments and is commonly used in orthopedic and spinal procedures due to its exceptional mechanical and biological properties, including bioactivity, biocompatibility, and suitability for replacing hard tissue. Advances in engineering and nanotechnology in healthcare and dentistry have further improved the application of polymers in dentistry, making them an excellent option for dental implants. This paper also provides an update on the antibacterial properties of polymers used in dentistry, utilizing advanced nanomaterials. The study used a liquid activator consisting of a mixture of sodium hydroxide (NaOH), a solution of sodium silicate (Na_2SiO_3), and silicon oxide (SiO_2) at different weight ratios, along with distilled water and standard Meta kaolinite weight, with a mixing time of 5 minutes. The geopolymer exhibited significant improvements in its properties with an increase in Si concentration until it reached the ideal geopolymer formula of 1Al-1Na-4Si. The geopolymer's compressive strength increased notably when the SiO_2 ratio was increased from 3.2 to 4.0. The highest compressive strength was observed with curing conditions of 25°C for 28 days, and the samples also had high density. The concentration of silica (from 3.2 to 4.0 molecular weight) in the general formula of geopolymer made of alkaline-based natural pure kaolinite, sodium silicate, and sodium hydroxide significantly affected mechanical and physical properties such as compressive strength and surface hardness. Therefore, these values should be considered standard for geopolymer production.

How to cite this article
Mohsien H A., Abdul Baqi H J. Effect of Si Concentration on Mechanical and Physical Properties of Nano-Size Alkaline-Based Pure Natural Kaolinite. J Nanostruct, 2023; 13(2):431-441. DOI: 10.22052/JNS.2023.02.013

INTRODUCTION

Implant-supported dental prostheses ensure the ability to evenly distribute the force of chewing over the underlying bony structure, which has an impact on the quality of life of edentulous patients [1]. The process of bone healing after implant placement depends on multiple factors and several stages until osteointegration occurs, which is characterized by intimate or direct contact between the bone and the implant surface [2]. Materials such as titanium and ceramics like zirconia are commonly used as dental implant materials due to their notable biocompatibility and mechanical properties [3, 4].

Additionally, according to Davidovits, geopolymer is an inorganic material of aluminum silicate activated by an alkaline activator solution [1, 5]. Geopolymers have promising mechanical properties such as compressive strength and excellent biological properties (biocompatible

* *Corresponding Author Email: hasanein.ali1101a@codental.uobaghdad.edu.iq*

material), making them suitable for safely replacing the bony structure [6]. Geopolymer is the amorphous structure of aluminum silicate produced from the polycondensation of its inorganic compounds, which are considered alkaline activated materials [7]. The geopolymer is formed through the reaction of aluminum silicate (kaolinite powder) with an alkaline activated liquid (sodium silicate, sodium hydroxide, silica gel or silica oxide, and distilled water) [8, 9]. Geopolymer, considered a polymeric material, could be useful in various applications, including using it for Portland cement, biological applications, industrial applications, and cosmetics [10]. Geopolymer is mainly used as an alkali-active material admixture as a binding medium that carries the inner aggregates to form a compact mass. This modified type of polymer has significant benefits such as high compressive strength, high-temperature resistance, and ideal chemical resistance. On the other hand, it is essential to protect the natural environment and use cleaner materials when possible [11].

The superior properties of geopolymer determine its broad application and development prospects, such as its use as a binder and repair material because of its low shrinkage and early strength [12]. In addition, geopolymer can be used as a coating material since it can be connected to the network structure of film material through the aluminum tetrahedral and silicon tetrahedral, thus providing a link of inorganic coating with non-toxic environmental protection [13, 14]. Geopolymer has also been used as a novel ceramic material that provides a new direct synthetic artificial structure or replica for biological uses because of its ability to form products with variable complex shapes and excellent performance [15]. Furthermore, kaolinite-based Na geopolymer is a biocompatible material that also possesses useful drug-carrying capacity with sufficient mechanical strength [16].

The synthesis of geopolymer involves dissolution, hydrolysis, and condensation of aluminate with silicate species to form a geopolymeric structure at room temperature [17]. Water is expelled from the reaction during the curing and extended drying processes, supporting the performance of geopolymers since water leaves the matrix forming a structure with nano-pores [18]. The geopolymerization setting process involves several chemical reactions, during which both the chemical and porous structures are formed. Thus, the porosity and chemical and mechanical properties of the materials are all affected by the geopolymerization reaction [19].

Regarding the mechanism of geopolymerization, it has been reported that geopolymerization begins with the dissolution stage, where the alumina-silica source is dissolved into silica monomers and alumina [20]. Later, the silica monomers are polymerized to the final geopolymer material after multiple continuous gelation and polymerization stages via dehydration reactions. The number and type of gels, as well as the polymer inter-phases, were examined by various studies and found.

In addition to evaluating the effect of silica ratio on the mechanical and physical properties of geopolymer, the aim of this study is to contribute to the optimization of geopolymer synthesis for dental implant applications. The novelty of this work lies in the investigation of the potential use of geopolymer as a dental implant material, which offers superior mechanical properties and biocompatibility compared to conventional materials. By optimizing the synthesis parameters, it is possible to tailor the properties of the geopolymer to meet the requirements for dental implant applications, such as high compressive strength, low shrinkage, and excellent wettability for improved bonding with bone tissue. The results of this study may pave the way for the development of a new generation of dental implants with improved performance and longevity.

MATERIALS AND METHODS

Materials and sample preparation

The kaolinite nanoparticles (particle size less than 100 nm) ($Al_2O_7Si_2$-$2H_2O$) used in this study were supplied by Sigma Aldrich, a German company, as a source of aluminum silicate (Si-Al) material. The powder was heated to 750°C for 3 hours with a temperature increase rate of about 5°C per 5 minutes. Sodium hydroxide, sodium silicate, and silica gel were also supplied by Sigma Aldrich.

X-ray diffraction (XRD) analysis

The material was characterized by an XRD analysis using a Cu Ka anode with a wavelength of 1.5406 A, a voltage of 40.0 Kv, a current of 30.0 mA, a scan range of 10.000° – 90.000° at 2θ range, a step size of 0.2000°, and a count time of 1.20 sec to detect the crystalline structure and purity. The XRD analysis data revealed that the kaolin

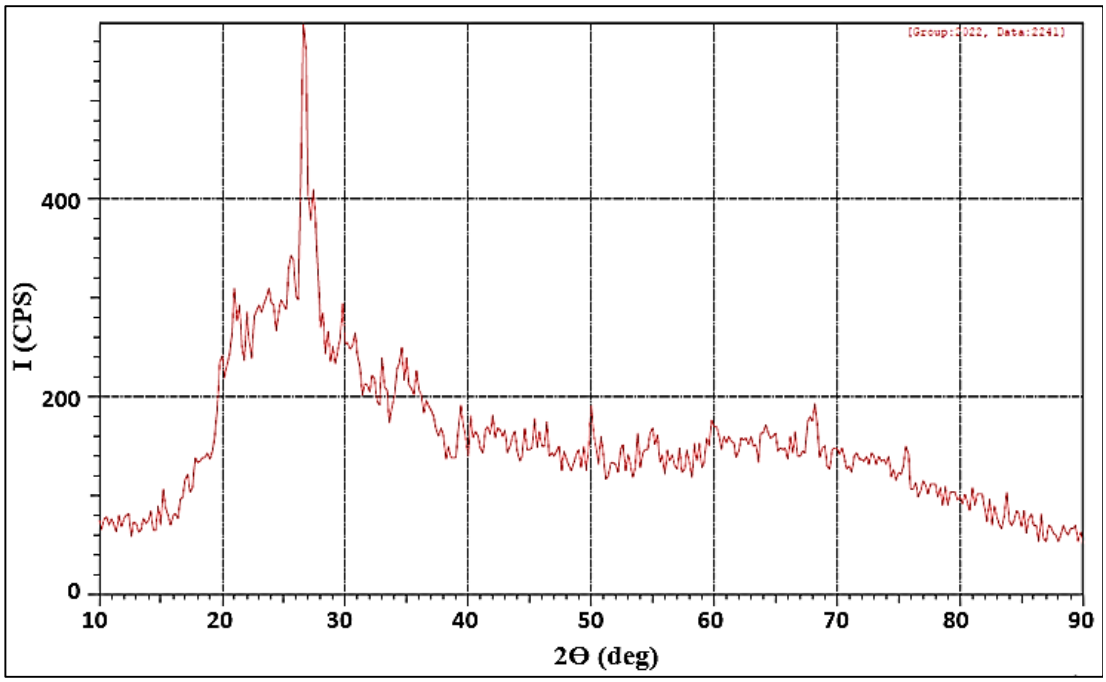

Fig 1. X-ray diffraction (XRD) analysis of kaolinite (Meta kaolinite)

powder was composed of kaolinite and quartz in the amorphous phase.

Samples preparation

Sodium hydroxide and sodium silicate were added to the water with continuous mixing until completely dissolved. Then, the temperature of the liquid was increased to ensure the dissolution of the silica gel. The liquid was left at room temperature for 24 hours to reach 25°C (see Table 1).

The meta kaolinite powder was added to the alkaline liquid in a plastic test tube, and the mixture was stirred for five minutes using an electric mixer at 5000 rpm. The resulting gel was then poured into a cylindrical mold with dimensions of 12.5 mm diameter and 25 mm height, and kept in an incubator to prevent water evaporation and sample contamination during geopolymerization. A total of 400 samples were prepared and divided into five groups, with each group containing eighty samples. Each group was further divided into two subgroups, with 40 samples tested after 14 days of polymerization and 40 samples tested after 28 days of polymerization. Each subgroup was then divided into four subgroups of ten samples for the following tests: Compressive strength, Diametral tensile strength, Surface hardness, Wettability.

Additional samples were also prepared for Scanning Electron Microscope (SEM) and Fourier-transform infrared spectroscopy (FTIR) analysis.

RESULT AND DISCUSSION

Scanning Electron Microscope (SEM):

Microstructure research was performed using a scanning electron microscope (SEM) of the inspect f50-FEI type with EDS at a magnification rate of 50-100,000x. The investigation involved previously prepared disk-shaped samples with dimensions of 12.5 mm in diameter and 2 mm in thickness.

The SEM micrographs of the top surface of the geopolymer indicated a compact morphology with a smooth surface and small spheroidal porosities. At very high magnification, some unreacted kaolinite crystals were observed, which might be remnants of the gelation process of the geopolymer. The presence of microcracks showed differences in the geopolymerization rate between the surface and the internal mass of the sample, where the surface was less polymerized due to water evaporation (Fig. 2A and B). The morphology demonstrated the dominant presence of

Table 1. The mixing molar ratio of the groups 1, 2, 3, 4, and 5

Basic GP components	Molecular Weight	The molar ratio of GP	Weight	M.wt%	
		Group 1+11ml distal water			
Na_2O	61.979	1	61.979	17.3996262	
Al_2O_3	101.961	1	101.961	28.6239419	10.73 Mata kaolinite
SiO_2	60.084	3.2	192.268	53.9764318	
		Group 2+11ml distal water			
Na_2O	61.979	1	61.979	16.831800	
Al_2O_3	101.96	1	101.961	27.689818	10.73 Mata kaolinite
SiO_2	60.084	3.4	204.285	55.478380	
		Group 3+11ml distal water			
Na_2O	61.979	1	61.979	16.2998655	10.73 Mata kaolinite
Al_2O_3	101.961	1	101.961	26.8147371	
SiO_2	60.084	3.6	216.3024	56.8853973	
		Group 4+11ml distal water			
Na_2O	61.979	1	61.979	15.8005217	10.73 Mata kaolinite
Al_2O_3	101.961	1	101.961	25.9932718	
SiO_2	60.084	3.8	228.319	58.2062065	
		Group 5+11ml distal water			
Na_2O	61.979	1	61.979	15.3308630	10.73 Mata kaolinite
Al_2O_3	101.961	1	101.961	25.2206413	
SiO_2	60.084	4.0	240.336	59.4484955	

unreacted kaolinite particles dispersed throughout the geopolymer matrix. This disaggregated morphology is a typical characteristic of fly ash-based geopolymers [21-23]. Furthermore, the globular morphology of the geopolymeric matrix was apparent at a magnification of 10,000x, and the particle dimensions ranged from 20 to 100 nm. The micrograph also revealed the appearance of white patches that represented an unselected scanning electron aggregation (Fig. 2C and D).

Fourier-transform infrared spectroscopy (FTIR).

The FTIR spectra of the geopolymer are presented in Fig. 3. Strong vibrational characteristics of aluminosilicates are observed. The peak positioned at around 953.44 cm^{-1} shifts to a lower value, which is characteristic of the geopolymerization reaction and corresponds to the vibration bands of Si-O-Al and Si-O-Si. The band at about 680 cm^{-1} is attributed to Si-OH bending vibration, while the absorption bands at 600-1100 cm^{-1} correspond to Al-O-Si vibrations [24]. The absorption band at around 1414.19 cm^{-1} is assigned to the stretching vibrations of CO_3^{2-} ions, indicating the presence of carbonate species [25]. Atmospheric CO_2 reacts with unhydrated sodium in the geopolymer to form sodium carbonate. A peak appearing at 1645.19 cm^{-1} is assigned to water. After the curing process, the intensity of these bands decreases in the geopolymer paste. Another explanation for the decrease in the OH bond may be attributed to the zeolite structure of zeolites (crystalline phase), which requires more molecules of water than the amorphous phase (mineral polymers). A single band is located at 1000 and 1004 cm^{-1} in all FTIR spectra, which corresponds to a region assigned to Si-O-Si [26, 27]. The asymmetric stretching of the O-C-O bonds of CO_3 may be due to atmospheric carbonation in all geopolymer matrices.

Compressive Strength

The compressive strength tests were conducted to evaluate the strength of the samples with varying concentrations of silicon oxide, and after two different geopolymerization periods, in accordance with the BS 1881-116:1983 standard, using mechanical testing with an atomic force max (Instron 5569, USA). The samples were compressed with a 50 kN pressing head at a speed of 5 mm/min. Fig. 4 shows the compressive strength results for the five groups with different Si concentrations and after 14 and 28 days of polymerization. The results indicate a significant increase in compressive strength between each group, with the fifth group (4.0 molecular weight SiO_2) exhibiting the greatest compressive strength, while the first group (3.2 molecular weight

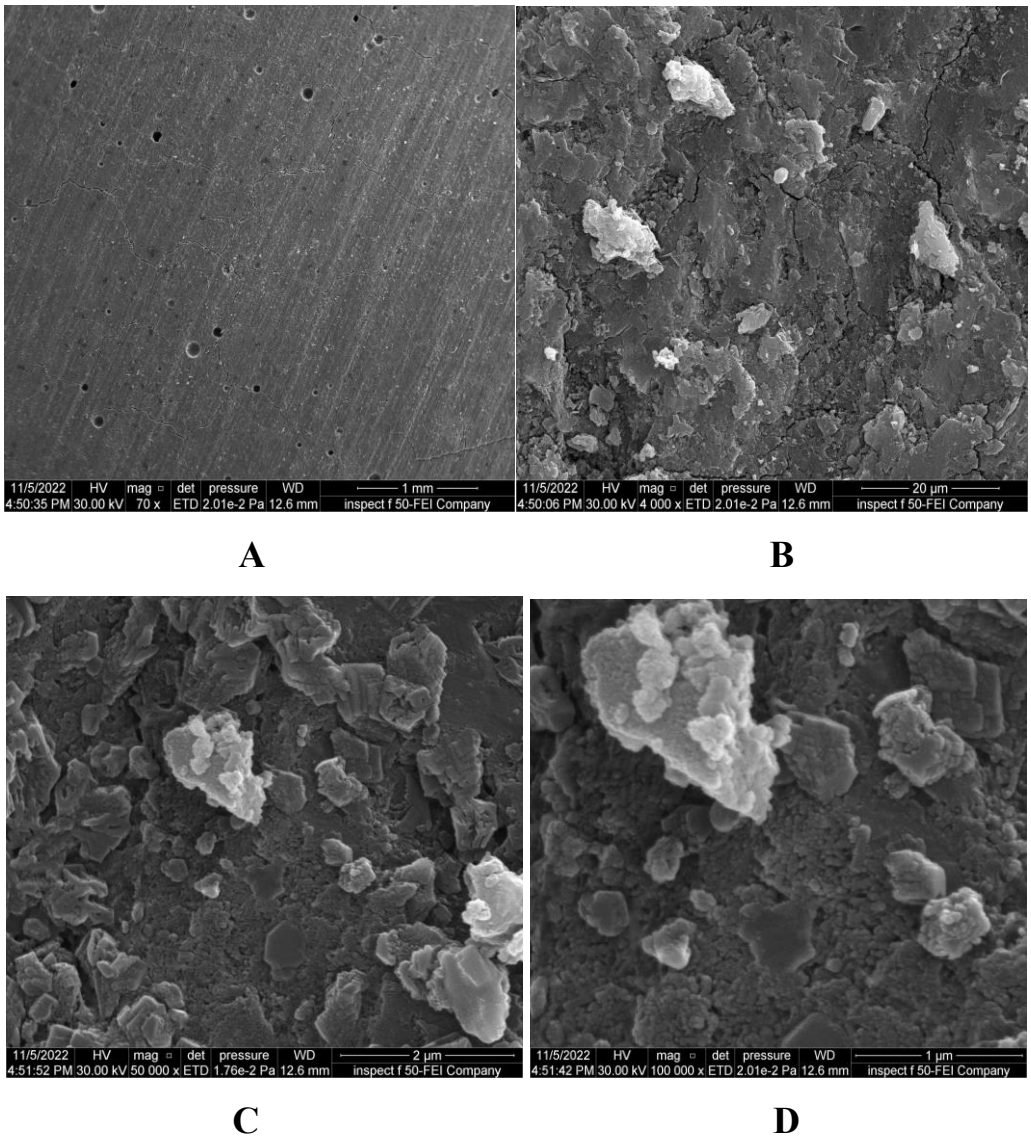

Fig. 2. Scanning Electron Microscope (SEM) of geopolymer (A) a compact morphology that only regular surface with the presence of small spheroidal porosities, (B) at very high magnification reveals some unreacted kaolinite crystals and, is probably reminiscent of the gelation process of the geopolymer. The presence of microcracks reveals the differences between the geopolymerization rate between the surface and the internal mass of the sample in which the surface is less polymerized due to water evaporation. (C) Presence of unreacted kaolinite particles that are well dispersed in the geopolymer matrix, and (D) at 10,000 magnification the particle dimensions are in the range of 20–100 nm, and the micrograph also reported the appearance of white patches

SiO_2) has the least strength. Mean, maximum, and minimum readings, p-values, and standard deviations are listed in Table 2.

The increase in the molecular weight percentage of silicon oxide leads to a higher dissolution of silica and alumina, resulting in the generation of more cations (SiO_4^+ and AlO_4^+). This contributes to the generation of new bonds during the gel-building phase of polysialate (-Si-O-Al-O-) which then upgrade to polysialate-siloxo (-Si-O-Al-O-Si-O-) as well as polysialate-disiloxo (Si-O-Al-O-Si-O-Si-O-) [28]. The strength improvement can be attributed mainly to the high SiO_2 content, which accounts for around 18.4% of the total geopolymer

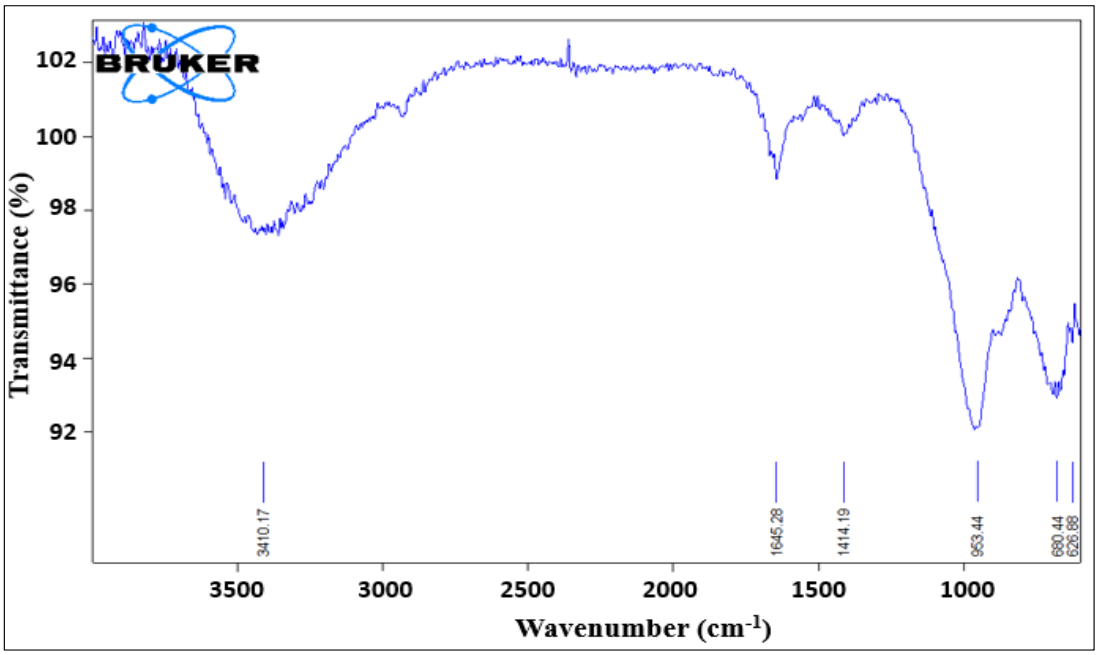

Fig. 3. Fourier-transform infrared spectrum (FTIR) of the geopolymer.

Table 2. presents a descriptive and statistical analysis of the compressive strength among different time periods and groups, according to the ANOVA test.

group	Time								F	P value*
	14-days				28-days					
	Mini	Maxi	Mean	±SD	Mini	Maxi	Mean	±SD		
3.2	32.60	34.40	33.64	0.723	51.20	59.100	55.00	2.341	1262.125	0.000
3.4	34.90	39.00	37.62	1.273	63.40	69.100	67.22	1.650	2423.724	0.000
3.6	41.40	43.50	42.33	0.591	66.60	69.400	68.31	0.985	1867.145	0.000
3.8	48.70	52.60	50.70	1.122	71.90	75.600	73.93	1.437	1492.788	0.000
4	50.00	53.20	52.11	1.215	84.10	88.400	87.22	1.269	3410.055	0.000
F		358.088				756.575				
P value*		0.000				0.000				

*=significant at p<0.05.

mass. Moreover, the dissolution of Si components results in the formation of Si-Al-Si gel and Si-O-Si gel due to the incorporation of Al^{3+} along with Si^{4+} and the activator solution, ultimately resulting in improved strength (Fig. 5) [29].

During the geopolymerization process, an amorphous or semi-crystalline polymeric resin is formed, which acts as a luting or adhesive to the aluminum silicate base component, making the material properties more suitable for the intended finished product. As a result, there is a significant increase in compressive strength after 28 days of polymerization compared to 14 days [23, 29]. Furthermore, the increase in compressive strength at different NaOH molarity over time can be attributed to the high dissolution of metakaolinite in the alkaline mixture, which accelerates the geopolymerization process, leading to earlier formation of geopolymer gels and a reduction in the setting time. Na^{+} also plays a role in the hardening stage, as shown in Fig. 5.

Therefore, a higher concentration of Na+ results in higher compressive strength of the geopolymer for a longer polymerization time [13].

Diametral tensile

The effect of increasing Si concentration in the general formula of geopolymer on the

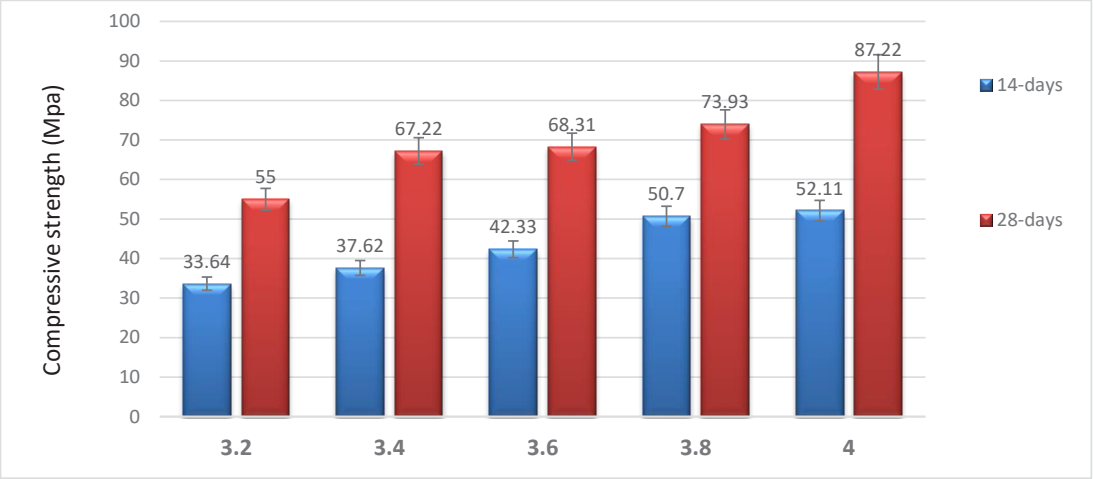

Fig. 4. Compressive strength of geopolymer among time and groups.

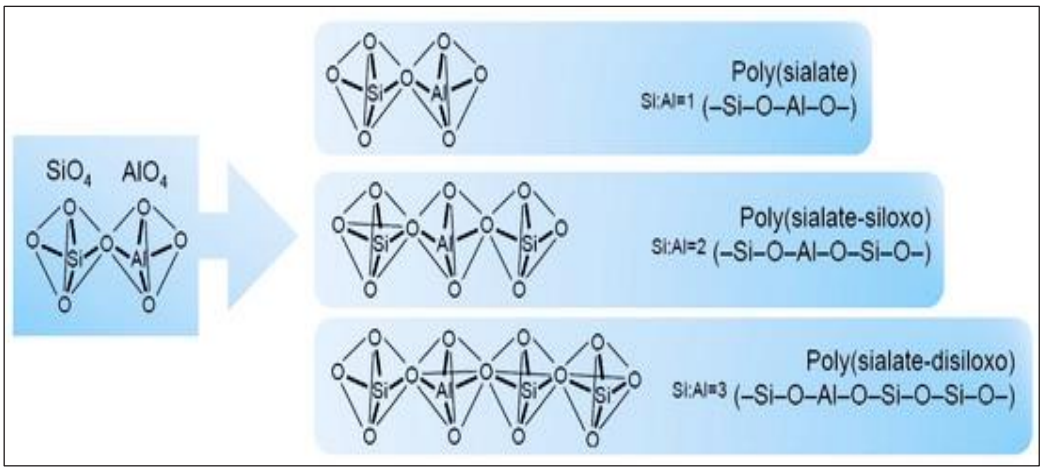

Fig. 5. Representation of oligomeric units of geopolymers according to the Davidovits model [28]

diametral tensile strength (length changes during compression before permanent or plastic deformation) is shown in Fig. 7. The results indicate that at each time of polymerization (14-day and 28-days), there is a significant increase in the percentage of elongation with an increase in Si concentration and polymerization time. The percentage of elongation is higher after 28 days compared to 14 days, with a significant difference. Mean, maximum, minimum, standard deviation, and p-value are shown in Table 3.

The experimental results suggest that an increase in Si concentration leads to a strength improvement, as it enhances the geopolymer mass by forming a larger and stronger chain of bonds. This improvement can be attributed to the high dissolution, condensation, and precipitation of Si-Al in the total geopolymer mass, which increases the workability and cohesiveness between the bands within the matrix [30].

Surface hardness (Vickers hardness)

The hardness values of all samples were measured using a Shimadzu Micro Vickers Hardness Tester from the HMV-G21ST series, with an indentation load of 300 gf on three different points for each sample. The surface hardness significantly increased with the increase of the Si

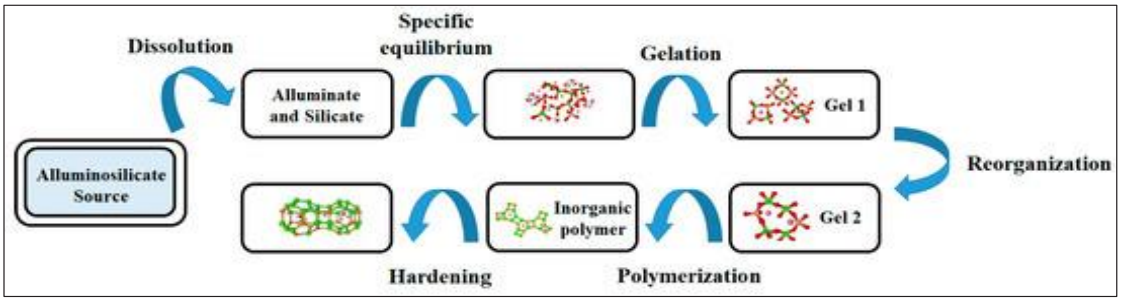

Fig. 6. Schematic representation of the geopolymerization mechanism.[29]

Table 3. Descriptive and statistical tests of the Percentage of Elongation among time and groups according to ANOVA test.

Groups	time								F	P value
	14-days				28-days					
	Mini	Maxi	Mean	±SD	Mini	Maxi	Mean	±SD		
3.2	0.010	0.030	0.019	0.009	0.200	0.500	0.390	0.099	106.108	0.000
3.4	0.010	0.030	0.020	0.008	0.500	0.900	0.765	0.160	427.871	0.000
3.6	0.010	0.030	0.019	0.009	0.800	0.950	0.845	0.060	525.970	0.000
3.8	0.100	0.300	0.200	0.082	0.800	0.950	0.915	0.053	394.106	0.000
4	0.100	0.300	0.210	0.088	0.900	1.200	1.020	0.092	505.790	0.000
F	15.694				89.475					
P value	0.000				0.000					

*=significant at p<0.05.

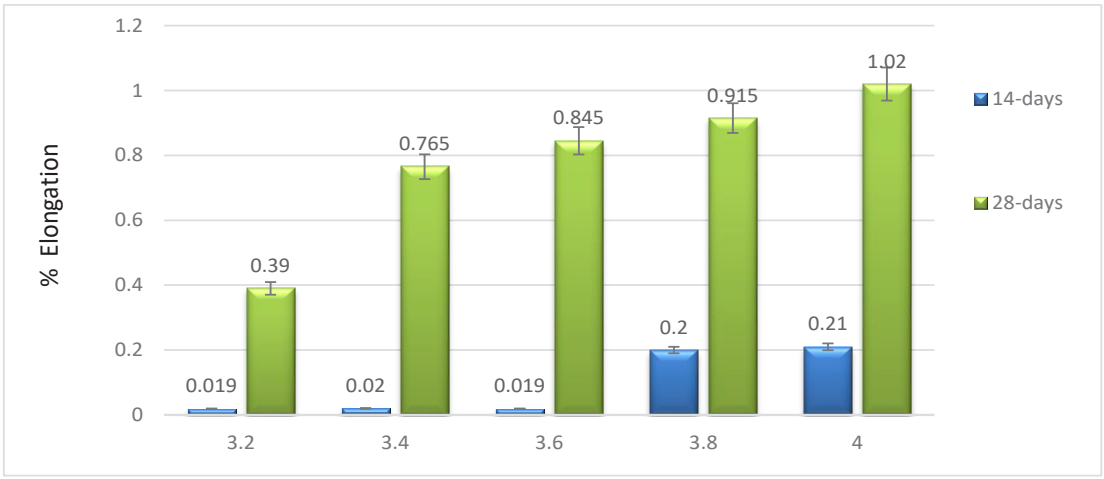

Fig. 7. Elongation among time and groups

ratio between each group. Group 5 exhibited the highest surface resistance due to the reduction of pore spaces. Surface damage was effectively minimized by decreasing porosities and voids, as the matrix became saturated with free Si ions reacting or forming a further polymerized chain, acting as an unreacted matrix nanofiller [31]. Fig. 8 shows the significant increase between each group and between the first and second polymerization times. Mean, maximum, minimum readings, standard deviation, and p-value were listed in Table 4.

Table 4. provides a descriptive and statistical test of Vickers hardness among time and groups according to the ANOVA test.

Groups	time								F	P value
	14-days				28-days					
	Mini	Maxi	Mean	±SD	Mini	Maxi	Mean	±SD		
3.2	22.200	27.500	25.290	1.788	54.800	58.400	56.510	1.141	1072.978	0.000
3.4	40.900	42.500	41.750	0.540	55.300	58.400	56.610	1.010	243.087	0.000
3.6	57.100	60.500	58.410	1.131	75.000	80.400	77.700	1.915	409.628	0.000
3.8	75.000	80.400	77.810	1.863	84.400	90.500	88.600	1.926	128.165	0.000
4	82.700	88.000	86.040	1.559	107.100	121.800	114.860	5.005	914.351	0.000
F		1383.073				1313.744				
P value		0.000				0.000				

*=significant at p<0.05.

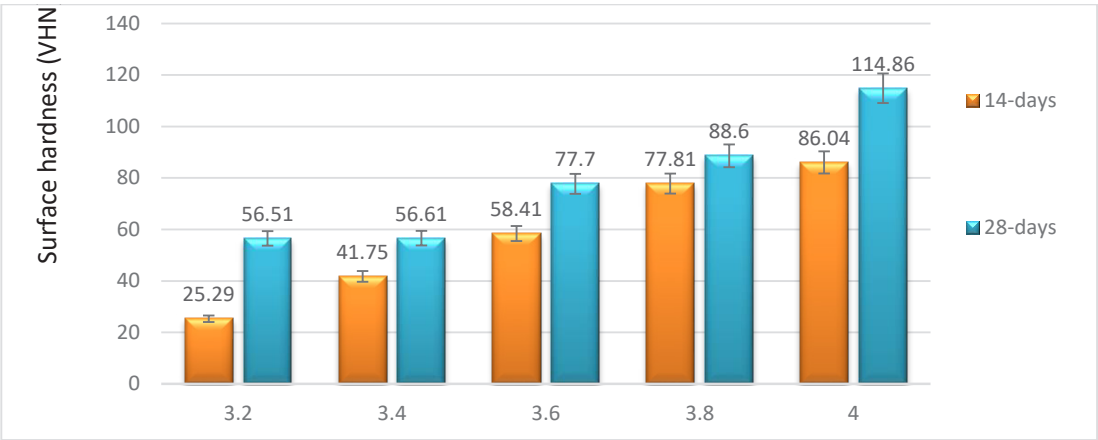

Fig. 8. Vickers hardness among time and groups.

Table 5. Descriptive and statistical tests of wettability among time and groups.

Groups	time								F	P value
	14-days				28-days					
	Mini	Maxi	Mean	±SD	Mini	Maxi	Mean	±SD		
3.2	15.990	16.300	16.15	0.085	6.450	6.940	6.763	0.198	16014.47	0.000
3.4	8.990	9.330	9.151	0.102	3.490	4.230	3.994	0.227	4826.206	0.000
3.6	4.990	5.670	5.352	0.222	3.220	3.640	3.541	0.125	595.180	0.000
3.8	2.470	2.780	2.699	0.102	2.120	2.980	2.479	0.233	8.783	0.004
4	0.480	0.570	0.519	0.030	0.340	0.990	0.756	0.192	10.193	0.002
F		13741.444				1766.152				
P value		0.000				0.000				

*=significant at p<0.05.

Wettability test

The wettability of geopolymer is influenced by surface properties and the component proportions. In general, a reduction in the contact angle results in better interconnection wettability. A contact angle below 25° is considered acceptable [30]. Fig. 9 shows the average contact angle for each group of kaolinite geopolymer. The best wettability is observed with the use of 4.0 mwt.% of Si, as Si is highly water absorbent and water-wettable material. The addition of reinforcement particulates improves the wettability until the optimum composition is achieved. An extremely high reinforcement percentage can further degrade the wettability of the composite solder, which can be worse than the monolithic alloy

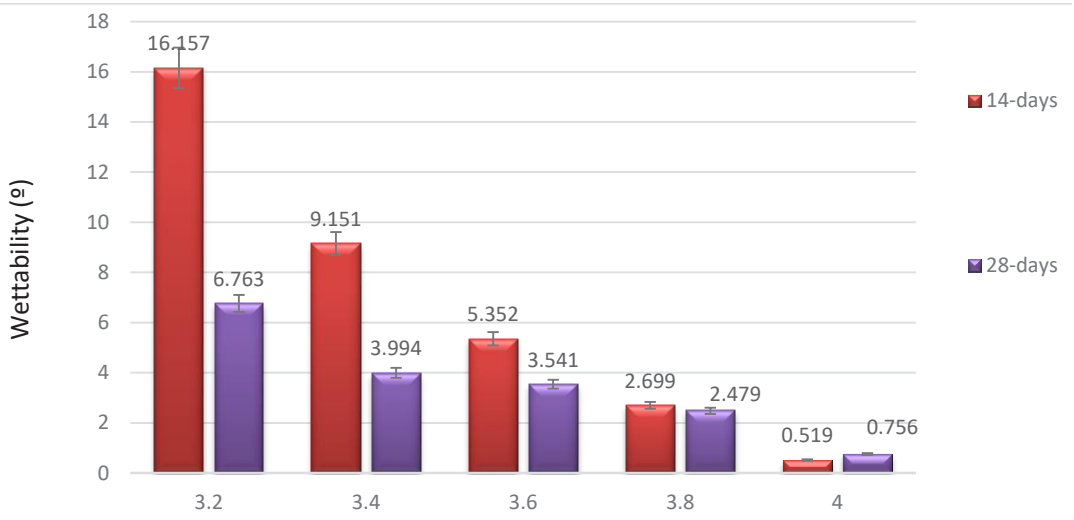

Fig. 9. Wettability among time and groups

of Sn-0.7Cu since ceramic-based reinforcement provides brittle properties [31]. Mean, maximum, and minimum readings, standard deviation, and p-value are listed in Table 5.

CONCLUSION

In conclusion, this study highlights the potential of geopolymer as a dental implant material due to its excellent mechanical and biological properties. With the advancement of engineering and nanotechnology, polymers have been improved as dental applications, and the results of this study provide valuable insights into the properties of geopolymer. The use of advanced nanomaterials has further enhanced the antibacterial properties of the polymer, making it an attractive option for dental implants. The study found that increasing the Si concentration in the geopolymer formula resulted in significant improvements in compressive strength and surface hardness. The ideal formula was found to be 1Al-1Na-4Si, and the samples cured at 25°C for 28 days had the highest compressive strength and density. It is essential to consider the material component proportion to achieve optimal properties. Geopolymer offers a promising alternative to traditional dental implant materials, and future studies should explore its potential further. Overall, the findings of this study suggest that geopolymer has great potential as a substitute for traditional dental implants, providing better mechanical and esthetic properties.

CONFLICT OF INTEREST

The authors declare that there is no conflict of interests regarding the publication of this manuscript.

REFERENCE

1. Azzawi ZGM, Hamad TI, Kadhim SA, Naji GA-H. Osseointegration evaluation of laser-deposited titanium dioxide nanoparticles on commercially pure titanium dental implants. J Mater Sci Mater Med. 2018;29(7).
2. Di Carlo S, De Angelis F, Brauner E, Rosella D, Papi P, Pompa G, et al. Histological and immunohistochemical evaluation of mandibular bone tissue regeneration. International Journal of Immunopathology and Pharmacology. 2018;32:205873841879824.
3. Gurusami K, Chandramohan D, Dinesh Kumar S, Dhanashekar M, Sathish T. Strengthening mechanism of Nd: Yag laser shock peening for commercially pure titanium (CP-TI) on surface integrity and residual stresses. Materials Today: Proceedings. 2020;21:981-987.
4. Sutanto D, Satari MH, Hernowo BS, Priosoeryanto BP, Septawendar R, Asri LATW, et al. In vivo histomorphologically evaluate of the initial bone healing in geopolymer-carbonated apatite nanocomposites as a potential dental implant material. Padjadjaran Journal of Dentistry. 2021;33(1):63.
5. Mackenzie KJD, Welter M. Geopolymer (aluminosilicate) composites. Advances in Ceramic Matrix Composites: Elsevier; 2014. p. 545-568.
6. Provis JL. Geopolymers and other alkali activated materials: why, how, and what? Mater Struct. 2013;47(1-2):11-25.
7. Al-Noor T, Ali A, Al-Sarray A, Al-Obaidi O, Obeidat A, Habash R. A Short Review: Chemistry of Curcumin and Its Metal Complex Derivatives. Journal of University of Anbar for Pure Science. 2022;16(1):20-26.
8. Provis JL, van Deventer JSJ. Geopolymers. Woodhead

Publishing Limited; 2009.
9. Al-Hawarin JI, Abu-Yamin A-A, Abu-Saleh AA-AA, Saraireh IAM, Almatarneh MH, Hasan M, et al. Synthesis, Characterization, and DFT Calculations of a New Sulfamethoxazole Schiff Base and Its Metal Complexes. Materials. 2023;16(14):5160.
10. Nasvi MCM, Rathnaweera TD, Padmanabhan E. Geopolymer as well cement and its mechanical integrity under deep down-hole stress conditions: application for carbon capture and storage wells. Geomechanics and Geophysics for Geo-Energy and Geo-Resources. 2016;2(4):245-256.
11. Zailan SN, Bouaissi A, Mahmed N, Abdullah MMAB. Influence of ZnO Nanoparticles on Mechanical Properties and Photocatalytic Activity of Self-cleaning ZnO-Based Geopolymer Paste. Journal of Inorganic and Organometallic Polymers and Materials. 2019;30(6):2007-2016.
12. Ibrahim SW, Rafeeq AK, Ahmedhamdi MS. Histomorphometric assessment of implant coated with mixture of nano-alumina and fluorapatite in rabbits. The Saudi Dental Journal. 2021;33(8):1142-1148.
13. Jo H, Lee S, Kim D, Lee J. Low Temperature Sealing of Anodized Aluminum Alloy for Enhancing Corrosion Resistance. Materials. 2020;13(21):4904.
14. Aguirre-Guerrero AM, Robayo-Salazar RA, de Gutiérrez RM. A novel geopolymer application: Coatings to protect reinforced concrete against corrosion. Applied Clay Science. 2017;135:437-446.
15. Sagoe-Crentsil K, Weng L. Dissolution processes, hydrolysis and condensation reactions during geopolymer synthesis: Part II. High Si/Al ratio systems. Journal of Materials Science. 2006;42(9):3007-3014.
16. Hardjito D, Wallah SE, Sumajouw DMJ, Rangan BV. Fly Ash-Based Geopolymer Concrete. Australian Journal of Structural Engineering. 2005;6(1):77-86.
17. Hu Z, Wyrzykowski M, Lura P. Estimation of reaction kinetics of geopolymers at early ages. Cem Concr Res. 2020;129:105971.
18. Nagel SM, Strangfeld C, Kruschwitz S. Application of H proton NMR relaxometry to building materials – A review. Journal of Magnetic Resonance Open. 2021;6-7:100012.
19. Davidovits J. Geopolymers. J Therm Anal. 1991;37(8):1633-1656.
20. van Riessen A, Chen-Tan N. Beneficiation of Collie fly ash for synthesis of geopolymer Part 2 – Geopolymers. Fuel. 2013;111:829-835.
21. Kaze RC, Beleuk à Moungam LM, Cannio M, Rosa R, Kamseu E, Melo UC, et al. Microstructure and engineering properties of Fe_2O_3(FeO)-Al_2O_3-SiO_2 based geopolymer composites. Journal of Cleaner Production. 2018;199:849-859.
22. Tahri W, Samet B, Pacheco-Torgal F, Aguiar J, Baklouti S. Geopolymeric repair mortars based on a low reactive clay. Eco-Efficient Repair and Rehabilitation of Concrete Infrastructures: Elsevier; 2018. p. 293-313.
23. Fernández-Jiménez A, Kovalchuk G, Palomo A. Activación alcalina de cenizas volantes. Relación entre el desarrollo mecánico resistente y la composición química de la ceniza. Materiales de Construcción. 2008;58(291).
24. Phair JW, Van Deventer JSJ. Effect of the silicate activator pH on the microstructural characteristics of waste-based geopolymers. Int J Miner Process. 2002;66(1-4):121-143.
25. Nakamoto K. Infrared and Raman Spectra of Inorganic and Coordination Compounds: Wiley; 2008 2008/04/30.
26. Davidovits J, Huaman L, Davidovits R. Ancient geopolymer in south-American monument. SEM and petrographic evidence. Mater Lett. 2019;235:120-124.
27. Kaze CR, Nana A, Lecomte-Nana GL, Deutou JGN, Kamseu E, Melo UC, et al. Thermal behaviour and microstructural evolution of metakaolin and meta-halloysite-based geopolymer binders: a comparative study. J Therm Anal Calorim. 2021;147(3):2055-2071.
28. Ye H, Zhang Y, Yu Z. Wood Flour's Effect on the Properties of Geopolymer-based Composites at Different Curing Times. BioResources. 2018;13(2).
29. Wongkvanklom A, Posi P, Kampala A, Kaewngao T, Chindaprasirt P. Beneficial utilization of recycled asphaltic concrete aggregate in high calcium fly ash geopolymer concrete. Case Studies in Construction Materials. 2021;15:e00615.
30. Mohammad MH, Al-Ghaban NMH. Histological and Histomorphometric Studies of the Effects of Hyaluronic Acid on Osseointegration of Titanium Implant in Rabbits. Journal of Baghdad College of Dentistry. 2018;30(2):10-16.
31. Abass SM. Surface Properties of Heat Treated with Different Durations of Titanium Alloy Dental Implants. Journal of Baghdad College of Dentistry. 2013;25(3):49-56.